NJC

ROYAL SOCIETY OF CHEMISTRY

COMMUNICATION

View Article Online
View Journal | View Issue

Cite this: *New J. Chem.*, 2022, **46**, 21995

Received 8th July 2022,
Accepted 20th October 2022

DOI: 10.1039/d2nj03367d

rsc.li/njc

Synthesis and functionalization of casein nanoparticles with aptamers for triple-negative breast cancer targeting†

Chiara Spanu,[a] Simona Camorani,[b] Silvia Tortorella,[ab] Lisa Agnello,[b] Mirko Maturi,[a] Mauro Comes Franchini,[a] Laura Cerchia *[b] and Erica Locatelli *[a]

This work shows the synthesis of a drug delivery system made of casein nanoparticles able to host hydrophobic molecules and be functionalized with aptamers targeting the epidermal growth factor receptor. *In vitro* cell viability and uptake analyses, performed on triple-negative breast cancer cells, confirmed the safety profile and the target selectivity.

The most studied types of nano-carriers for nano-medical applications in drug delivery systems have been biodegradable polymers that could either be natural or synthetic but, in general, with the latter being more easily processed for the development of tailored systems with a wide range of properties.[1–3] On the other hand, natural polymers have great potential for their intrinsic properties, such as biodegradability, bio-compatibility, and non-toxicity.[4] Food proteins, a natural class of macromolecules, represent one of the most interesting nanocarriers investigated so far.[5,6] Thanks to their low immunogenicity, amphiphilic character, and easy modification of exposed functional groups, they could be easily employed for addressing the issues of nano-systems for medical applications.[7] Several systems based on food proteins such as albumin, gelatin, collagen, zein, or casein have been studied and synthesized to deliver drugs, nutrients, and probiotic organisms.[8–10] Casein is the most abundant protein in milk, along with β-lactoglobulin. Its isoelectric point is at pH 4.6, whereas its alkaline forms such as sodium caseinate (NaCas) are completely soluble in water.[11] What makes casein unique and interesting for pharmaceutical applications in drug delivery systems is its natural properties of being a transporter of essential micronutrients, such as calcium and phosphate,[12,13] thanks to its ability to self-assemble into a micellar structure with a hydrophobic core and a hydrophilic surface. This self-assembling ability makes casein an excellent material for encapsulating hydrophobic substances and protect them from oxidation,[7] UV light[14] or temperature.[15,16] Only few and recent works aimed at the preparation of drug delivery systems based on casein nanomicelles.[17–19] Overall, these studies highlight that casein is perfectly able to encapsulate hydrophobic drugs in nanomicelles with improved stability, solubility, and bioavailability, but often requires complex and invasive techniques such as microfluidization and spray drying for their manufacture. More importantly, no studies have yet extended the drug delivery system towards chemical targeting.[20] Aptamers are short oligonucleotide sequences of RNA or DNA, which fold into unique three-dimensional structures and bind targets with high affinity and specificity. They represent a new emergent class of components that find their application in chemical targeting.[21] Cancer treatments have been the most investigated area for the application of highly specialized aptamer-based drug delivery systems.[22] Like antibodies, aptamers are highly selective to cancer cell-surface receptors, but offer great advantages over antibodies for targeted cancer therapy such as cost- and time-effective discovery, easy synthesis and modification, and very high thermal stability. Furthermore, they have a small size for effective tumor penetration and possess no or low immunogenicity.[23] Among the various cancer types, many studies were dedicated to investigate the possibility of active targeting of triple-negative breast cancer (TNBC). TNBC is one of the most aggressive subtypes of breast cancer that still lacks an efficacious therapy, due to the lack of receptors for progesteron, estrogen, or HER2/neu.[24] The CL4 nuclease-resistant 2′-fluoro-pyrimidine (2′-F-Py) containing RNA aptamers is an ideal candidate for TNBC-active targeting.[25] It binds to domain IV in the epidermal growth factor receptor (EGFR) extracellular region and its binding to EGFR-positive cancer cell lines correlates with the expression's level of the receptor on the cell surface, while it does not bind to EGFR-negative non tumor

[a] *Department of Industrial Chemistry "Toso Montanari", University of Bologna, Viale Risorgimento 4, 40136, Bologna, Italy. E-mail: erica.locatelli2@unibo.it*
[b] *Institute of Experimental Endocrinology and Oncology "Gaetano Salvatore", CNR, Via S. Pansini 5, 80131 Naples, Italy. E-mail: cerchia@unina.it*

† Electronic supplementary information (ESI) available. See DOI: https://doi.org/10.1039/d2nj03367d

fibroblasts.[26] Because of its high affinity to the surface of cells belonging to different tumor types, including TNBC, CL4 has been extensively used as a component of novel nanoformulations for cancer therapy.[21,27] EGFR is frequently overexpressed in both primary and metastatic TNBC.[28] We previously demonstrated the exquisite selectivity of CL4 for EGFR-positive TNBC cells both *in vitro* and in preclinical mouse models.[27,29] The present research explores for the first time the functionalization of the hydrophilic surface of casein nanoparticles (CNPs) with aptamers to address the selectivity of the system towards TNBC cells, thus ensuring active targeting and high internalization of lipophilic drugs into the cell compartments, while limiting the toxicity of the nanocarrier itself. CNPs encapsulating 5,5-difluoro-5*H*-4λ5-dipyrrolo[1,2-*c*:2′,1′-*f*][1,3,2]diazaborinin-4-ylium-5-uide (BODIPY) as a model lipophilic compound (BODIPY@CNPs) were synthesized using mild conditions achieving a controlled size and polydispersity index (PDI). The model drug delivery system functionalized with CL4-aptamers was thus analyzed *in vitro* using MDA-MB-231 and BT-549 cells in order to evaluate the effectiveness of the targeting, for the ability of our casein-aptamer system to deliver lipophilic compounds, such as BODIPY, inside the tumor cells, thus opening the way to further and deeper studies.

Casein solubility is strongly dependent on the pH, temperature, and ionic strength and it is affected also by the presence of calcium or phosphate ions.[30] Near the isoelectric point (pI 4.6), casein is completely insoluble, while moving away from it the solubility increases. This occurs because around pH 5 the functional groups present on the protein have a neutral overall charge, causing aggregation and precipitation of the protein. Moving towards higher or lower pH, the external functional groups become negatively/positively charged.[31] Consequently, not only the repulsion between protein chains increases but also the dispersion is improved. In this work, a synthetic procedure to dissolve casein was adopted. Following the addition of sodium hydroxide until pH 8 to an aqueous suspension of casein, a significant increase in the solubility was recorded as a result of the deprotonation of acidic moieties in casein. Furthermore, soluble sodium caseinate (NaCas) obtained may be in equilibrium with its aggregated form, nano-micelles. The fabrication of casein nanoparticles starts using lyophilized NaCas, eventually a lipophilic compound and an aqueous solution of calcium chloride (1 M). After less than one hour at 30 °C, the mixture was emulsified with a trip probe sonicator and the final CNPs are obtained. Indeed, the addition of calcium chloride solution causes a rearrangement of the NaCas towards a more packed state as a result of the electrostatic interactions established between Ca^{2+} ions and phosphoserine residues present in the hydrophilic side of the protein.[19,32,33] Two different types of CNPs were synthesized and characterized: CNPs and BODIPY@CNPs. The BODIPY dye was chosen and added to allow better traceability and quantification of nanoparticles during *in vitro* release tests. Furthermore, BODIPY is a lipophilic compound and we report an easy methodology to entrap it efficiently. Finally, after purification of the obtained CNPs, the conjugation of the amino-terminated CL4 aptamer for each sample was performed. Due to the activation of casein's carboxylic acid *via* EDC/NHS chemistry and the thermal activation of the aptamers, amide bonds between the aptamer's amine group and casein's carboxylic acid may form. The same synthetic procedure was used to conjugate CNPs with CL4-scrambled to be used as a negative control (Fig. 1 and Fig. S1, ESI†). All the details of the materials, experimental procedures and set-ups are available in the ESI.† All samples were purified and then characterized by dynamic light scattering (DLS) at a constant pH of 6.5–7.0 in water. As shown in Table 1, the nanoparticles display a reproducible hydrodynamic diameter that does not exceed over 200 nm, even after the aptamer's conjugation. Comparing the empty nanomicelles to BODIPY@CNPs_CL4 or BODIPY@CNPs_SCR, there is an increase in size, which may be due to the dye encapsulation (more details in Fig. S2 and S3, ESI†). Furthermore, a low polydispersity index (PDI), which reveals a homogeneous size distribution and negative ζ-potential values, due to negatively charged groups on the protein's surface, was achieved. Together these results provide significant evidence of the

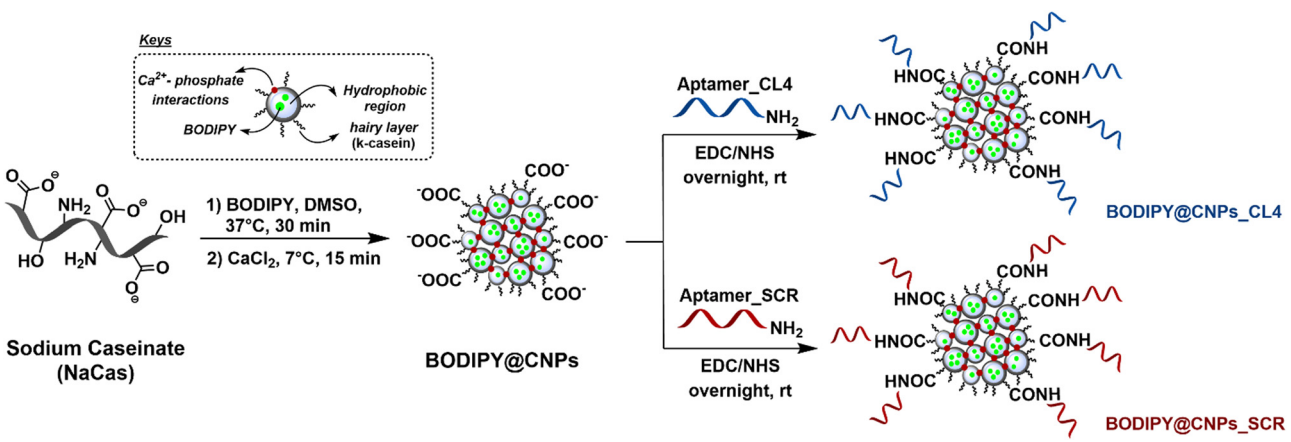

Fig. 1 Schematic representation of the development of casein aptamer-based nanoparticles with encapsulated BODIPY: BODIPY@CNPs_CL4 and BODIPY@CNPs_SCR.

Table 1 Summary of the characterization of the proposed nanosystems. Size, PDI and ζ-potential were determined by DLS; the total dry matter was measured by drying at 120 °C 1 mL of NP solution. BODIPY concentration was determined by UV-Vis. EE% = encapsulation efficiency; LC% = loading capacity

Samples	Size (nm)	PDI	ζ-Pot (mV)	Dry matter (mg mL^{-1})	[BODIPY] (mM)	BODIPY EE%	BODIPY LC%
CNPs@CL4	156 ± 5	0.197	−13.3	17.0	—	—	—
CNPs@SCR	167 ± 3	0.212	−13.8	16.0	—	—	—
BODIPY@CNPs_CL4	194 ± 9	0.244	−12.1	16.0	0.163	43.6	0.25
BODIPY@CNPs_SCR	189 ± 8	0.237	−13.1	15.5	0.201	53.6	0.32

homogeneity of the particles in terms of size, surface charge and suitability of the particles for *in vivo* experiments. Encapsulation efficiency (EE%) and loading capacity (LC%) were determined *via* UV-VIS analysis (more details are in the ESI† and Fig. S4). EE% expresses the percentage of dye that is effectively trapped in the CNPs, while LC% expresses the mass percentage of the dye relative to the total nanosystem mass (Table 1). We should underline that the observed values are derived from a two-step reaction: nanoparticle synthesis and aptamer conjugation. For this reason, the results obtained had to be considered more than satisfactory and in line with the features required to perform *in vitro* cellular tests. ATR-FTIR analysis was performed on freeze-dried samples to explore the chemical features of the different preparations (Fig. 2a). The FTIR spectra of all systems show two characteristic bands for amide at 1635 cm^{-1} corresponding to the C═O stretching vibration of amide I and at 1513 cm^{-1} corresponding to the N–H bending vibration of amide II. These signals are related to the protein's peptide bond and their maintenance during later stages suggests that casein was not damaged. Furthermore, at around 3247 cm^{-1} and 2949 cm^{-1} are shown the stretching vibrations of −OH/−NH and of aliphatic C–H, respectively. To see the distribution and morphology of particles, the SEM images were acquired. As shown in Fig. 2b, c and Fig. S4, ESI,† both CNPs and BODIPY@CNPs exhibit a homogeneous distribution and size with a globular shape. These images additionally support the presence of nano-vectors perfectly suitable for drug delivery application.

To assess the CL4 aptamer-mediated delivery of nanoparticles to cancer cells, the human EGFR-positive MDA-MB-231 cell line was chosen because it represents an established model for the mesenchymal stem-like TNBC and well recapitulates the high malignant and invasive phenotype of this poorly differentiated subtype.[34] Importantly, we have already demonstrated that CL4 not only binds to EGFR on the cell surface, but also is rapidly internalized into MDA-MB-231 cells both in a nude form[29] and conjugated to polymeric nanoparticles,[27,35] or antibodies.[36] The specificity of the cellular uptake of the nanovectors was assessed in EGFR-depleted MDA-MB-231 cells (MDA-MB-231 EGFR-KO), which represent the more appropriate negative control to validate the targeting specificity of an aptamer against its cell surface receptor.[37] Thus, cultured MDA-MB-231 and MDA-MB-231 EGFR-KO cells were treated with BODIPY@CNPs_CL4 or BODIPY@CNPs_SCR for 40 min at 37 °C and then washed to remove unbound nanoparticles. Cell nuclei and membranes were stained with DAPI and WGA-647, respectively. Confocal microscopy revealed a clear nanoparticle-associated fluorescence signal within the cytoplasm of MDA-MB-231 cells, but not MDA-MB-231 EGFR-KO, treated with the CL4-equipped CNPs (Fig. 3a and Fig. S5a, ESI†). No signal was observed in both cell lines upon treatment with the SCR-nanoparticles, indicating that CNP internalization is specifically driven by the CL4 aptamer into EGFR-positive TNBC cells. Furthermore, the flow cytometry assays revealed that according to the efficient recognition of EGFR-positive BT-549 TNBC cells by CL4,[27,29,35] the aptamer induces a strong uptake of CNPs into these cells (Fig. 3b). As a final test, the safety profile of the nanocarrier conjugated with the aptamer was checked: no cytotoxicity of unloaded CNPs conjugated to either CL4 or SCR aptamers was observed at 0.1 mg ml^{-1} and 0.2 mg ml^{-1} (Fig. S5b, ESI†).

Conclusions

In conclusion, an easy and versatile method for casein-based nanocarrier preparation and drug loading has been developed.

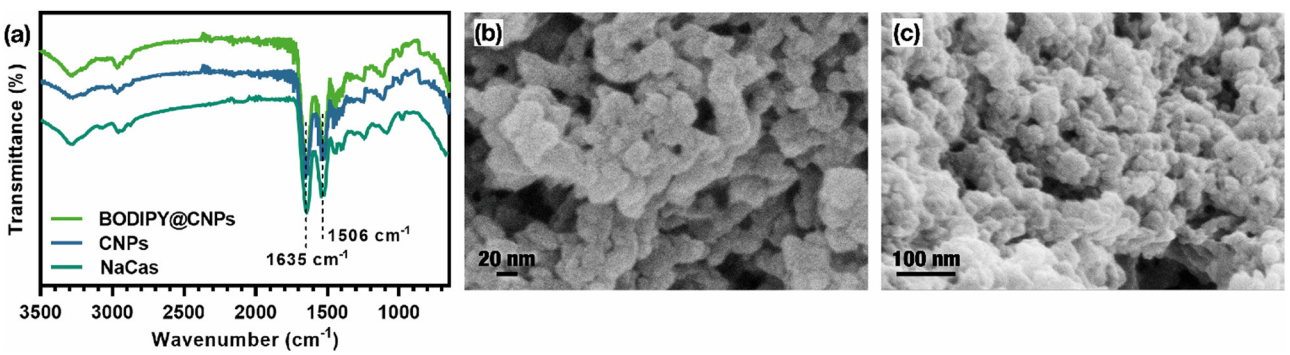

Fig. 2 Characterization of BODIPY nanoparticles: the ATR-FTIR analysis (a) and FEG-STEM images of CNPs (b) and BODIPY@CNPs (c).

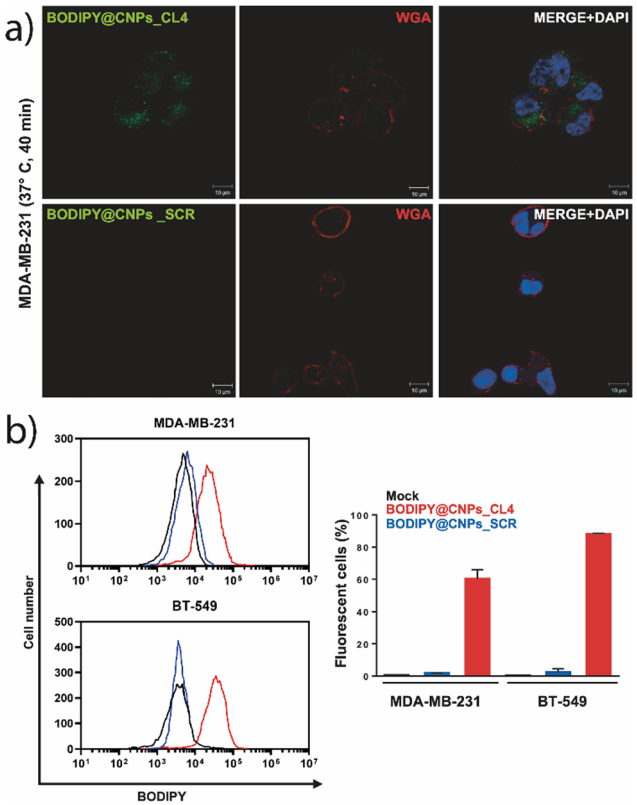

Fig. 3 *In vitro* cell uptake of CL4-conjugated nanoparticles. (a) Representative confocal images of MDA-MB-231 cells treated with BODIPY@CNPs_CL4 or BODIPY@CNPs_SCR at 37 °C for 40 min. Red: cell membranes; blue: nuclei; and green: nanoparticles. Scale bars, 10 μm. All digital images were captured at the same setting to allow direct comparison of staining patterns. (b) Representative flow cytometry analysis of MDA-MB-231 and BT549 cells treated with BODIPY@CNPs_CL4 or BODIPY@CNPs_SCR for 40 min at 37 °C. Data are expressed as percentage of fluorescent cells, as calculated by BD Accuri C6 Software with respect to mock-treated cells. Bars depict mean ± SD of three independent experiments.

Casein showed promising peculiarity in terms of safety and high lipophilic compound payloads as well as the possibility to surface functionalization: indeed, CL4-aptamer was conjugated onto the external surface of the nanocarrier, thus increasing the targeting ability and internalization in EGFR-positive triple-negative breast cancer MDA-MB-231 and BT-549 cells.

Author contributions

Conceptualization: EL and LC. Data curation: LA, MM, and ST. Formal analysis: CS and SC. Funding acquisition: MCF and LC. Investigation: CS and LA. Methodology: CS and MM. Supervision: EL and ST. Writing – original draft: CS and LA. Writing – review and editing: EL, MCF, and LC.

Conflicts of interest

There are no conflicts to declare.

Acknowledgements

The University of Bologna is gratefully acknowledged. This research was partially funded by Fondazione AIRC per la Ricerca sul Cancro (IG 23052) to LC.

Notes and references

1 S. Tortorella, V. Vetri Buratti, M. Maturi, L. Sambri, M. Comes Franchini and E. Locatelli, *Int. J. Nanomed.*, 2020, **15**, 9909–9937.
2 A. Kumari, S. K. Yadav and S. C. Yadav, *Colloids Surf., B*, 2010, **75**, 1–18.
3 S. Tortorella, M. Maturi, F. Dapporto, C. Spanu, L. Sambri, M. Comes Franchini, M. Chiariello and E. Locatelli, *Cellulose*, 2020, **27**, 8503–8511.
4 H. Chen, H. Wooten, L. Thompson and K. Pan, in *Biopolymer Nanostructures for Food Encapsulation Purposes*, Elsevier, 2019, pp. 39–68.
5 A. O. Elzoghby, W. M. Samy and N. A. Elgindy, *J. Controlled Release*, 2012, **161**, 38–49.
6 E. Assadpour and S. Mahdi Jafari, *Crit. Rev. Food Sci. Nutr.*, 2019, **59**, 3129–3151.
7 M. Haham, S. Ish-Shalom, M. Nodelman, I. Duek, E. Segal, M. Kustanovich and Y. D. Livney, *Food Funct.*, 2012, **3**, 737.
8 Y. Qin, L. Xu, Y.-Y. Guan and H. Liu, *ACS Appl. Bio Mater.*, 2020, **3**, 3196–3202.
9 D. Lickorish, J. A. M. Ramshaw, J. A. Werkmeister, V. Glattauer and C. R. Howlett, *J. Biomed. Mater. Res.*, 2004, **68A**, 19–27.
10 T. K. Głąb and J. Boratyński, *Top. Curr. Chem.*, 2017, **375**, 71.
11 Y. Liu and R. Guo, *Biophys. Chem.*, 2008, **136**, 67–73.
12 P. F. Fox and A. Brodkorb, *Int. Dairy J.*, 2008, **18**, 677–684.
13 F. Song, L.-M. Zhang, J.-F. Shi and N.-N. Li, *Colloids Surf., B*, 2010, **79**, 142–148.
14 A. O. Elzoghby, W. S. Abo El-Fotoh and N. A. Elgindy, *J. Controlled Release*, 2011, **153**, 206–216.
15 Y. Zhang, S. He, Y. Ma, W. Xu and H. Tang, *RSC Adv.*, 2015, **5**, 77595–77600.
16 A. Matalanis, O. G. Jones and D. J. McClements, *Food Hydrocolloids*, 2011, **25**, 1865–1880.
17 B.-S. Chu, S. Ichikawa, S. Kanafusa and M. Nakajima, *J. Am. Oil Chem. Soc.*, 2007, **84**, 1053–1062.
18 A. O. Elzoghby, M. W. Helmy, W. M. Samy and N. A. Elgindy, *Pharm. Res.*, 2013, **30**, 2654–2663.
19 K. C. Barick, A. Tripathi, B. Dutta, S. B. Shelar and P. A. Hassan, *J. Pharm. Sci.*, 2021, **110**, 2114–2120.
20 J. M. Morachis, E. A. Mahmoud and A. Almutairi, *Pharmacol. Rev.*, 2012, **64**, 505–519.
21 S. Shigdar, L. Agnello, M. Fedele, S. Camorani and L. Cerchia, *Pharmaceutics*, 2021, **14**, 28.
22 F. He, N. Wen, D. Xiao, J. Yan, H. Xiong, S. Cai, Z. Liu and Y. Liu, *Curr. Med. Chem.*, 2020, **27**, 2189–2219.
23 S. Camorani, E. Crescenzi, M. Fedele and L. Cerchia, *Biochim. Biophys. Acta, Rev. Cancer*, 2018, **1869**, 263–277.
24 S. Camorani, M. Fedele, A. Zannetti and L. Cerchia, *Pharmaceuticals*, 2018, **11**, 123.

25 C. L. Esposito, D. Passaro, I. Longobardo, G. Condorelli, P. Marotta, A. Affuso, V. de Franciscis and L. Cerchia, *PLoS One*, 2011, **6**, e24071.
26 S. Camorani, E. Crescenzi, D. Colecchia, A. Carpentieri, A. Amoresano, M. Fedele, M. Chiariello and L. Cerchia, *Oncotarget*, 2015, **6**, 37570–37587.
27 L. Agnello, S. Tortorella, A. D'Argenio, C. Carbone, S. Camorani, E. Locatelli, L. Auletta, D. Sorrentino, M. Fedele, A. Zannetti, M. C. Franchini and L. Cerchia, *J. Exp. Clin. Cancer Res.*, 2021, **40**, 239.
28 R. Costa, A. N. Shah, C. A. Santa-Maria, M. R. Cruz, D. Mahalingam, B. A. Carneiro, Y. K. Chae, M. Cristofanilli, W. J. Gradishar and F. J. Giles, *Cancer Treat. Rev.*, 2017, **53**, 111–119.
29 S. Camorani, E. Crescenzi, M. Gramanzini, M. Fedele, A. Zannetti and L. Cerchia, *Sci. Rep.*, 2017, **7**, 46659.
30 E. D. Strange, D. L. Van Hekken and V. H. Holsinger, *J. Dairy Sci.*, 1994, **77**, 1216–1222.
31 A. E. Post, B. Arnold, J. Weiss and J. Hinrichs, *J. Dairy Sci.*, 2012, **95**, 1603–1616.
32 D. J. McMahon and B. S. Oommen, *Advanced Dairy Chemistry*, Springer US, Boston, MA, 2013, pp. 185–209.
33 F. Rehan, N. Ahemad and M. Gupta, *Colloids Surf., B*, 2019, **179**, 280–292.
34 S. Camorani, B. S. Hill, F. Collina, S. Gargiulo, M. Napolitano, M. Cantile, M. Di Bonito, G. Botti, M. Fedele, A. Zannetti and L. Cerchia, *Theranostics*, 2018, **8**, 5178–5199.
35 L. E. Ibarra, S. Camorani, L. Agnello, E. Pedone, L. Pirone, C. A. Chesta, R. E. Palacios, M. Fedele and L. Cerchia, *Pharmaceutics*, 2022, **14**, 626.
36 M. Passariello, S. Camorani, C. Vetrei, L. Cerchia and C. De Lorenzo, *Cancers*, 2019, **11**, 1268.
37 M. McKeague, V. Calzada, L. Cerchia, M. DeRosa, J. M. Heemstra, N. Janjic, P. E. Johnson, L. Kraus, J. Limson, G. Mayer, M. Nilsen-Hamilton, D. Porciani, T. K. Sharma, B. Suess, J. A. Tanner and S. Shigdar, *Aptamers*, 2022, 10–18.